Energy storage participation for frequency regulation of microgrid in PV-dominated power system

Nirdesh Singh, Dinesh Kumar Jain
Department of Electrical Engineering, Deenbandhu Chhotu Ram University of Science and Technology, Sonipat, India

Article Info	ABSTRACT
	The frequency stability of a power grid is effectively managed through the inertia and power reserves supplied by synchronous generators. Due to increasing concerns about the greenhouse effect and global warming, renewable energy sources (or microgrids) are increasingly replacing traditional fossil fuel-based methods of electricity generation. As microgrid deployment proliferates, power systems' inherent complexity and non-linear dynamics have escalated, rendering conventional controllers inadequate across diverse operating conditions. Factors such as reduced energy inertia, heightened penetration of renewable energy sources, and significant power fluctuations within confined transmission systems have heightened the vulnerability of microgrid frequencies to instability. This paper elucidates the concept of microgrids, examines frequency fluctuations in the presence of solar and diesel generators alongside load variations, and presents simulation-based analyses. Moreover, it provides a succinct overview of frequency control methodologies. Validation outcomes demonstrate the efficacy of the proposed controller in maintaining system frequency amidst fluctuating load demands and renewable energy inputs.

Corresponding Author:

Nirdesh Singh
Department of Electrical Engineering, Deenbandhu Chhotu Ram University of Science and Technology
Murthal, Sonipat, Haryana, India
Email: singh.niru28@gmail.com

1. INTRODUCTION

In recent years, there has been a growing imperative to transition towards generating electrical power from renewable energy resources (RESs), propelled by the depletion of traditional fossil fuel reserves [1]. This transition has led to an increasing integration of RESs into conventional electricity grids, thereby decentralizing bulk power production. However, this integration introduces challenges associated with variability and disturbances stemming from the inherent unpredictability of RESs and distributed generators (DGs). Moreover, the expansion of electrical networks and transmission lines to serve remote electrical loads escalates the costs of electricity production and transmission, exacerbated by increasing demand. To address the constraints associated with integrating RESs/DGs into the grid, the concept of a microgrid (MG) has emerged as a viable solution [2]. A microgrid is characterized as a low-voltage network integrating numerous small-scale distributed energy generation and storage units [3], [4]. It functions in dual modes: interconnected with the primary grid and independently isolated from it. Typically, the microgrid is linked to the national grid, yet during emergencies marked by significant disruptions, it autonomously disconnects from the main grid. This enables it to exclusively supply power to critical local loads, ensuring their continued operation [5], [6]. Introducing this concept into power systems aims to enhance reliability, flexibility, and adaptability while addressing economic and environmental challenges inherent in conventional power systems.

According to the International Energy Agency (IEA), global energy demand continues to rise with economic and technological advancements [7]. Currently, conventional energy generators constitute the primary source of meeting this global energy demand. However, the finite nature of non-renewable fossil fuels leads to their gradual depletion, with well-documented adverse environmental consequences [8].

Figure 1(a) demonstrates the worldwide new installation of RES for the years 2013–2019 [9]. System operators worldwide are exploring various renewable energy sources (RES), including solar, wind, biomass, hydro, geothermal, and ocean power, to meet the energy demands stipulated by respective regulatory bodies. Wind power plants and grid-connected solar photovoltaic (PV) have emerged as up-and-coming options. Moreover, renewable energy sources (RES) have the potential to meet the growing global power demand. It is projected that within the next 30 years, Denmark's power system will achieve 100% RES penetration. The European Union, The United States, and China have also established ambitious targets for integrating RES into their power systems. Current renewable penetration levels and future targets for several countries are illustrated in Figure 1(b) [9]. This figure indicates that Ireland, China, Spain, India, and Europe plan to incorporate more than 90% renewable resources into their power systems by 2050.

The proliferation of microgrids within power systems has fundamentally altered operational dynamics. Consequently, this has induced heightened complexity and non-linearity within power networks. Managing microgrid (MG) operations in islanded mode presents greater complexity compared to network-connected mode. Moreover, within islanded microgrids incorporating renewable sources like wind and solar energy, fluctuations in wind speed and variations in solar radiation intensity present substantial energy perturbations to the microgrid. Hence, addressing frequency deviations within islanded microgrids stands out as a paramount control challenge in microgrid research.
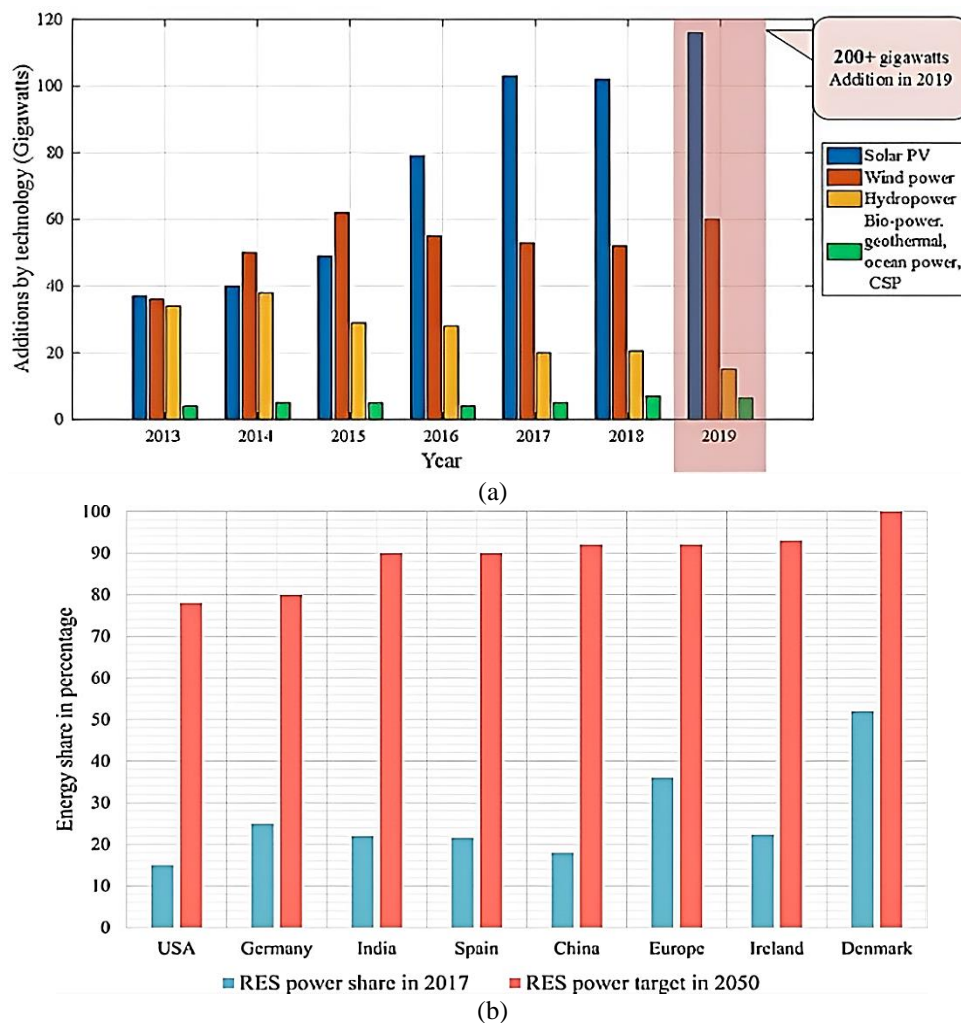

(a)

(b)

Figure 1. The global installation and future target installation of RES: (a) worldwide year-wise installation of RES and (b) current and future targets of renewable penetration level

Numerous references have investigated and presented diverse methodologies for microgrid frequency control, focusing on optimizing controller parameters through metaheuristic algorithms. Previous studies [10], [11] employ PI control and proportional-integral-derivative (PID) controllers, respectively. In [12], the particle swarm optimization (PSO) algorithm is employed, whereas in [13], the spider social behavior (SSO) algorithm is utilized for the optimization of PID control parameters. Additionally, it employs the harmonic search (HS) algorithm for load-frequency control. Abazari et al. [14] introduces a fuzzy controller with coefficients optimized using the PSO algorithm. Furthermore, model predictive control (MPC) is explored for load-frequency control in [15], [16], while Abazari et al. [17] utilizes a fuzzy controller to regulate the frequency of a multi-microgrid system. Leng et al. [18] introduces a two-level model predictive control (MPC) approach, as well as multiple MPC control strategies in [19], while Zhang et al. [20] presents an MPC-based method for coordinated control of wind turbine blades and electric hybrid vehicles aimed at mitigating power fluctuations and enhancing microgrid frequency stability. Conversely, Khodja et al. [21] delves into the Ziegler-Nichols-based PID method (ZN-PID), while Zaheeruddin [22] scrutinizes the fractional-order-based PID method (FOPID), and Oshnoei et al. [23] suggests the implementation of fuzzy control-based fractional-order PID (fuzzy FOPID). Additionally, Khosravi et al. [24] utilizes a kriging-based surrogate fractional-order PID method for control system design. To enhance the set point of active power and bolster frequency stability in islanded microgrids (MGs), virtual inertia control is implemented, leveraging the rate of change of frequency (RoCoF) function [25], [26]. Investigation into the frequency stability of an autonomous microgrid (MG) system, as documented in [27], employed a coefficient diagram approach alongside a PID accelerator controller. A comparative analysis of published PID and 2DoF-PID controllers was conducted to evaluate performance. Gheisarnejad and Khooban [28] deliberated on designing a fuzzy PID controller for a multi-microgrid system as a secondary control mechanism. Additionally, Patel et al. [29] implemented a fuzzy tilt integral derivative controller to enhance frequency stability within a hybrid microgrid (MG), demonstrating superior performance through comparative analysis against classical PID controllers. Moreover, Khokhar et al. [30] introduced the slap swarm optimization (SSO) technique-adjusted cascade (PI-PD) controller, tailored for regulating system frequency in an MG integrated with an electric vehicle, showcasing innovative advancements in control strategy. Zand et al. [31] and Baldinelli et al. [32] introduce a novel approach to multi-objective optimization for scheduling distributed energy resources (DERs) within microgrids. Similarly, in [33], the focus shifts to energy management within an isolated microgrid, emphasizing maximizing DER utilization while minimizing operational costs. Nonetheless, these references overlook the substantial impacts of abrupt load fluctuations or unpredictable changes in renewable energy sources (RES) power output during microgrid resource planning.

2. RESEARCH OBJECTIVE (INTELLECTUAL CONTRIBUTION)

The extensive integration of renewable energy sources (RES) worldwide has significantly altered power system dynamics. Traditionally, the kinetic energy stored in the rotating mass of synchronous generators (SGs) has been relied upon to compensate for generation deficits. However, with the widespread adoption of RES, conventional SGs are being displaced. RES installations typically lack inherent system inertia, necessitating additional control mechanisms to ensure stability. Consequently, the overall system inertia is diminishing, rendering low-inertia power systems more susceptible to various disturbances and uncertainties inherent in modern power grids. Challenges associated with low inertia grids include heightened rates of frequency change, increased frequency deviation, and distributed photovoltaic (PV) trip events, among others. The objective of this paper is to counter these challenges and to regulate the frequency of the system by controlling the active power of the battery.

The rest of the manuscript is organized as follows: the second section outlines the microgrid's architecture and its corresponding model, along with the modelling of the battery. Following this, section 3 offers insight into the simulation implementation and presents the results of frequency control within the microgrid under investigation. Lastly, the conclusion and future recommendations are provided in the fourth section of the article.

3. MODELLING OF THE STORAGE SYSTEM WITH METHODOLOGY TO CONTROL FREQUENCY

The modeling process enhances understanding of battery behavior and plays a crucial role in improving overall system performance and efficiency. Batteries are crucial as versatile energy storage solutions, catering to various applications with varying power demands. These devices are indispensable across numerous industries, utilized in both series and parallel setups to accommodate specific load requirements. Battery modeling is a potent technique for predicting and enhancing key parameters, such as state of charge, battery longevity, and charge/discharge behavior. Lithium-ion batteries hold particular prominence among

battery types due to their lightweight design, high-energy density, and minimal self-discharge rates, offering significant advantages in various contexts. A precise electrical equivalent model, such as the resistor-capacitor (RC) circuit battery block illustrated in Figure 2, becomes essential for conducting thorough analyses and making informed decisions regarding system design and operation. To calculate the combined voltage of the battery network:

$$V_T = E_m - I_{batt}R_0 - \sum_1^n V_n \tag{1}$$

$$V_n = \int_0^t \left[\frac{I_{batt}}{C_n} - \frac{V_n}{R_n C_n}\right] dt \tag{2}$$

$$SOC = \frac{-1}{C_{batt}} \int_0^t I_{batt}\, dt \tag{3}$$

$$I_{batt} = \frac{I_{in}}{N_p} \tag{4}$$

$$V_{out} = N_s V_T \tag{5}$$

$$P_{BattLoss} = I_{batt}^2 R_0 + \sum_1^n \frac{V_n^2}{R_n} \tag{6}$$

$$P_{LossBatt} = -(I_{batt}^2 R_0 + \sum_1^n \frac{V_n^2}{R_n}) \tag{7}$$

$$P_{StoreBatt} = P_{LossBatt} + P_{batt} \tag{8}$$

$$Ld_{AmpHr} = \int_0^t I_{batt}\, dt \tag{9}$$

where SOC is a state of charge; E_m is battery open-circuit voltage; I_{batt} is per module battery current; I_{in} is the total current flowing from the battery network; R_0 is series resistance; N_p is no. of parallel branches; V_{out}, V_T is a combined voltage of the battery network; V_n is a voltage of nth RC pair; R_n is the resistance of the nth RC pair; C_n is the capacitance of nth RC pair; C_{batt} is battery capacity; P_{batt} is battery power; $P_{BattLoss}$ is battery network power loss; $P_{LossBatt}$ is negative of battery network power loss; $P_{StoreBatt}$ is battery network power stored; and T is battery temperature. Positive current indicates battery discharge and negative current indicates battery charge. The (1) to (9) has been used for the modeling of the battery.

Waveforms for battery state of charge (SOC), current, and voltage are shown in Figure 3. In Figure 3(a), the state of charge (SOC) of the battery is depicted at 50% initially, with a charging process initiated at 3 seconds into the simulation. Throughout the duration of the simulation, the battery's SOC increases marginally from 47.9% to 48.02%. Figure 3(b) illustrates the battery's current profile, indicating a state of zero current prior to 3 seconds. Subsequently, post the 3-second mark, the battery begins charging at a rate of 30 kW, corresponding to a current of -200 A. Figure 3(c) demonstrates a voltage increase occurring precisely at 3 seconds, stabilizing at 262 V for the duration of the simulation.
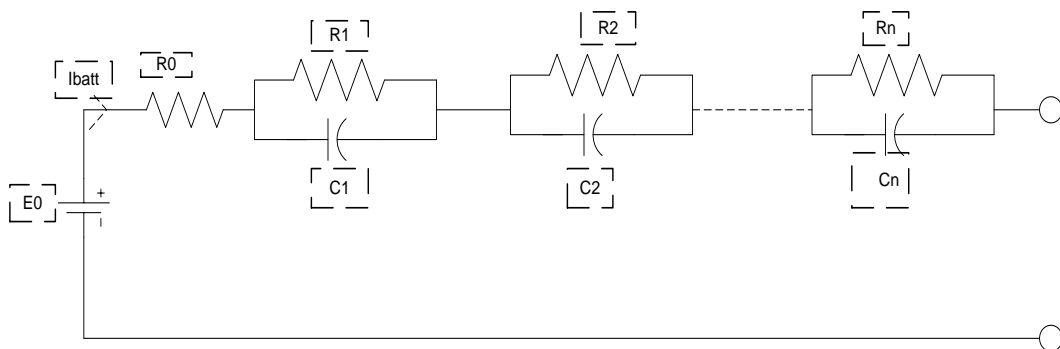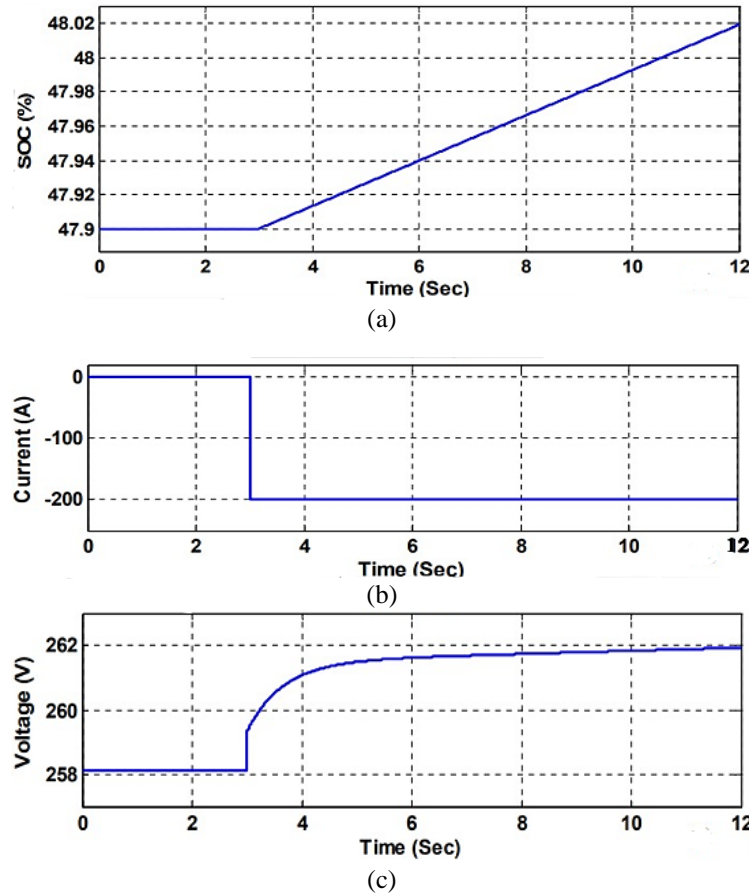

Figure 2. Equivalent model of battery

Figure 3. Battery waveforms: (a) battery SOC, (b) battery current, and (c) battery voltage

The proposed system's numerous components are represented to create a full model. The control scheme depicted in Figure 4 is primarily utilized to derive reference source currents, which are then employed in the battery energy storage system (BESS) VSI's pulse width modulation (PWM) current controller. There are two components to the reference source currents: an in-phase component and a quadrature component. The in-phase component of the reference source currents is required to charge the battery of BESS and/or to feed active power to the load. This active power component may be kept constant to generate constant power at the point of common coupling (PCC). The surplus power is absorbed by the BESS and during peaking load BESS replenishes the increased requirement of load resulting in frequency regulation. Here, the active component of the source current remains fixed, whereas the reactive power component depends upon the requirement of AC terminal voltage control. Such controllers based on BESS, in addition, perform the tasks of frequency and voltage control in case of unbalanced and non-linear loads. This has been shown in (10) to (24).

They are estimated in the following order: the unit vectors in phase with Va, Vb, and Vc are derived as in (10).

$$U_a = \frac{v_a}{v_m}; U_b = \frac{v_b}{v_m}; U_c = \frac{v_c}{v_m} \tag{10}$$

Where V_m is the amplitude of the AC terminal voltage at the PCC and can be calculated as (11).

$$V_m = \frac{2}{3} \sqrt{(V_a{}^2 + V_b{}^2 + V_c{}^2)} \tag{11}$$

Where Va, Vb, and Vc are the instantaneous voltages at PCC and can be derived as:

$$V_a = V_{san} - R_s i_{sa} - L_s P i_{sa}, V_b = V_{sbn} - R_s i_{sb} - L_s P i_{sb}, \ V_c = V_{scn} - R_s i_{sc} - L_s P i_{sc}$$

where P represents the time differential operator (d/dt) and L_s and R_s are per phase source inductance and resistance, respectively. V_{san}, V_{sbn}, and V_{scn} are the three-phase instantaneous input supply voltages at PCC and are expressed as (12).

$$V_{san} = V_m \sin(\omega t); \quad V_{sbn} = V_m \sin(\omega t - 2\pi/3); \quad V_{scn} = V_m \sin(\omega t + 2\pi/3) \tag{12}$$

The peak value, denoted as V_m, and the angular frequency ($\omega = 2\pi f$) of the power supply are established parameters in this context. The derivation of unit vectors orthogonal to V_a, V_b, and V_c involves implementing a quadrature transformation on the in-phase unit vectors U_a, U_b, and U_c as (13)-(15).

$$W_a = -U_b / \sqrt{3} + U_c / \sqrt{3}, \tag{13}$$

$$W_b = \sqrt{3}\, U_a / 2 + (U_b - U_c)/(2\sqrt{3}), \tag{14}$$

$$W_c = -\sqrt{3}\, U_a / 2 + (U_b - U_c)/(2\sqrt{3}) \tag{15}$$

The quadrature component of the reference source currents is computed as follows. The voltage error V_{er} at PCC at the nth sampling instant is as (16).

$$V_{er(n)} = V_{ref(n)} - V_{m(n)} \tag{16}$$

3.1. Modelling of BESS

The BESS is operated in current-controlled mode, and the volt-current equations are calculated as illustrated in Figure 4.

$$V_{ab} = R_c i_{ca} + L_c P i_{ca} + e_{ab} - R_c i_{cb} - L_c P i_{cb} \tag{17}$$

$$V_{bc} = R_c i_{cb} + L_c P i_{cb} + e_{bc} - R_c i_{cc} - L_c P i_{cc} \tag{18}$$

Further:

$$i_{ca} + i_{cb} + i_{cc} = 0 \tag{19}$$

to calculate Pi_{ca} and Pi_{cb}, use (17) to (19).

$$Pi_{ca} = \{(V_{bc} - e_{bc}) + 2(V_{ab} - e_{ab}) - 3R_{ca}i_{ca}\}/3L_c = 0 \tag{20}$$

$$Pi_{cb} = \{(V_{bc} - e_{bc}) - (V_{ab} - e_{ab}) - 3R_{ca}i_{cb}\}/3L_c = 0 \tag{21}$$

From (19), i_{cc} can be expressed as (22).

$$i_{cc} = -(i_{ca} + i_{cb}) \tag{22}$$

The DC bus voltage derivation can be expressed as:

$$PV_{dc} = i_{ca} S_A + i_{cb} S_B + i_{cc} S_C - i_{bb})/C_{dc} \tag{23}$$

where i_{bb} is the battery's charging/discharging current. SA, SB, and SC are switching functions that specify the ON/OFF states of the BESS VSI bridge switches S_1-S_6. The inverter's AC output voltages are represented in the three-phase PWM AC voltages e_a, e_b, and e_c of the BESS. AC line voltages of BESS are:

$$e_{ab} = V_{bc}(S_A - S_B), \quad e_{bc} = V_{bc}(S_B - S_C), \quad e_{ca} = V_{bc}(S_C - S_A) \tag{24}$$

for the ON and OFF conditions of the upper and lower switches of the phase 'a' leg of the VSI bridge, the switching function SA has values of 0 and 1, respectively. The other phase lags follow a similar rationale. The battery is modelled by using Thevenin's equivalent circuit model.
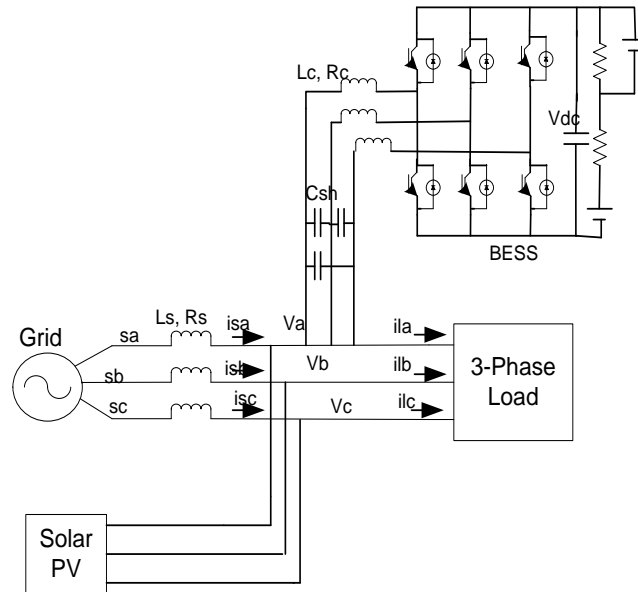
Figure 4. Principle of control

4. RESULTS AND DISCUSSION

In Figure 5, following a 12-second simulation, the frequency exhibits drop to 59.68 Hz, 59.80 Hz, and 59.77 Hz at 0.5 seconds, 3 seconds, and 4.5 seconds, respectively. These reductions are attributed to additional loads of 50 kW, 30 kW, and 50 kW, respectively, in addition to the existing load of 100 kW. At 4.5 seconds, the battery begins discharging at a rate of 50 kW to meet the heightened demand, resulting in a frequency decline to 59.75 Hz.

In Figure 6, following a 12-second simulation, there is an initial decrease in frequency to 59.68 Hz at 0.5 seconds, attributed to an additional load of 50 kW. A subsequent drop occurs at 3 seconds, resulting in a further load increase of 30 kW. At the 3-second mark, the battery begins charging at a rate of 30 kW, causing the frequency to decline to 59.92 Hz. Subsequently, the frequency stabilizes at 59.92 Hz
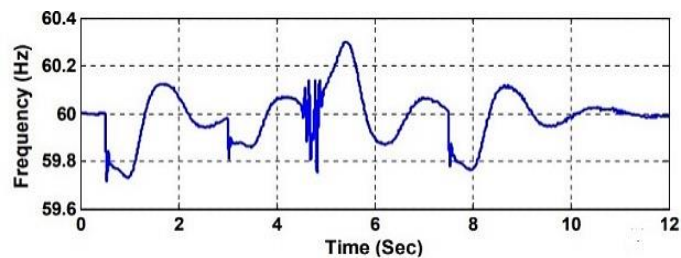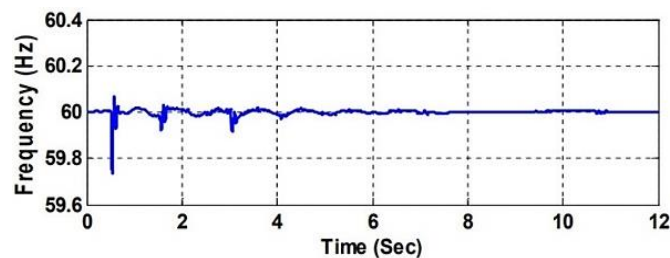

Figure 5. Frequency at load bus without any controller

Figure 6. Frequency at load bus with controller

5.   CONCLUSION

Maintaining a balance between active power production and consumption stands as a pivotal factor in guaranteeing frequency stability within microgrid systems. This paper delves into the concept of microgrids and examines the frequency fluctuation dynamics under the influence of solar, diesel generators, and load variations, subsequently simulating these scenarios. Brief discussions on frequency control methodologies are provided, showcasing the suitability and precision of the proposed controller. Finally, the simulation outcomes under various perturbations demonstrate the effective performance of the proposed control system.

REFERENCES

[1]   D. Zhou, A. Al-Durra, K. Zhang, A. Ravey, and F. Gao, "Robust prognostic indicator for renewable energy technologies: A novel error correction grey prediction model," *IEEE Transactions on Industrial Electronics*, vol. 66, no. 12, pp. 9312–9325, 2019, doi: 10.1109/TIE.2019.2893867.

[2]   T. Kerdphol, F. S. Rahman, Y. Mitani, M. Watanabe, and S. K. Küfeoğlu, "A robust virtual inertia control of an islanded microgrid considering high penetration of renewable energy," *IEEE Access*, vol. 6, pp. 625–636, 2017, doi: 10.1109/ACCESS.2017.2773486.

[3]   F. Hardan, R. Norman, and W. Leithead, "Model-based control of a VSC-based power generator with synthetic inertia provision in an isolated micro-grid," *IET Generation, Transmission & Distribution*, vol. 14, no. 12, pp. 5037–5046, 2020, doi: 10.1049/iet-gtd.2020.0304.

[4]   J. Li, S. Chen, C. Jiang, F. Liu, and W. Xiao, "Adaptive dynamic programming approach for micro-grid optimal energy transmission scheduling," in *2020 39th Chinese Control Conference (CCC)*, 2020, pp. 1–6, doi: 10.23919/CCC50068.2020.9189579.

[5]   P. C. Sahu, R. C. Prusty, and S. Panda, "Frequency regulation of an electric vehicle-operated micro-grid under WOA-tuned fuzzy cascade controller," *International Journal of Ambient Energy*, vol. 43, no. 5, pp. 1–18, 2020, doi: 10.1080/01430750.2020.1783358.

[6]   L. Reed, M. Dworkin, P. Vaishnav, and M. G. Morgan, "Expanding Transmission Capacity: Examples of Regulatory Paths for Five Alternative Strategies," *The Electricity Journal*, vol. 33, no. 6, p. 106770, 2020, doi: 10.1016/j.tej.2020.106770.

[7]   L. Cozzi *et al.*, "World Energy Outlook 2020," *Energy*, vol. 30, 2019.

[8]   R. A. Ristinen, J. J. Kraushaar, and J. T. Brack, *Energy and the Environment*, 4th ed., Hoboken, New Jersey, USA: Wiley, 2022.

[9]   M. N. H. Shazon, N. A. Masood, and A. Jawad, "Frequency control challenges and potential countermeasures in future low-inertia power systems: A review," *Energy Reports*, vol. 8, pp. 6191–6219, 2022, doi: 10.1016/j.egyr.2022.04.063.

[10]   A. Garces, "Small-signal stability in island residential microgrids considering droop controls and multiple scenarios of generation," *Electric Power Systems Research*, vol. 185, p. 106371, 2020, doi: 10.1016/j.epsr.2020.106371.

[11]   A. Annamraju and S. Nandiraju, "Frequency control in an autonomous two-area hybrid microgrid using grasshopper optimization-based robust PID controller," *2018 8th IEEE India International Conference on Power Electronics (IICPE)*, 2018, pp. 1–6, doi: 10.1109/IICPE.2018.8709428.

[12]   D. Mishra, P. C. Nayak, and R. C. Prusty, "PSO optimized PIDF controller for Load-frequency control of AC Multi-Islanded-Micro grid system," in *2020 International Conference on Renewable Energy Integration into Smart Grids: A Multidisciplinary Approach to Technology Modelling and Simulation (ICREISG)*, 2020, pp. 116–121, doi: 10.1109/ICREISG49226.2020.9174552.

[13]   I. Abdulwahab, S. A. Faskari, T. A. Belgore, and T. A. Babaita, "An improved hybrid micro-grid load frequency control scheme for an autonomous system," *FUOYE Journal of Engineering and Technology*, vol. 6, no. 4, pp. 369–374, 2021, doi: 10.46792/fuoyejet.v6i4.698.

[14]   A. Abazari, M. G. Dozein, and H. Monsef, "A new load frequency control strategy for an AC micro-grid: PSO-based Fuzzy logic controlling approach," in *2018 Smart Grid Conference (SGC)*, 2018, pp. 1–7, doi: 10.1109/SGC.2018.8777791.

[15]   V. P. S. R. V. R. S. Sesha and S. S. Kesanakurthy, "Model predictive control approach for frequency and voltage control of standalone micro-grid," *IET Generation, Transmission & Distribution*, vol. 12, no. 4, pp. 3405–3413, 2018, doi: 10.1049/iet-gtd.2017.0804.

[16]   S. A. Ghorashi Khalil Abadi, S. I. Habibi, T. Khalili, and A. Bidram, "A model predictive control strategy for performance improvement of hybrid energy storage systems in DC microgrids," *IEEE Access*, vol. 10, pp. 25400–25421, 2022, doi: 10.1109/ACCESS.2022.3155668.

[17]   A. Abazari, H. Monsef, and B. Wu, "Coordination strategies of distributed energy resources including FESS, DEG, FC and WTG in load frequency control (LFC) scheme of hybrid isolated micro-grid," *International Journal of Electrical Power & Energy Systems*, vol. 109, pp. 535–547, 2019, doi: 10.1016/j.ijepes.2019.02.029.

[18]   M. Leng, C. Zheng, T. Dragicevic, G. Zhou, F. Blaabjerg, and J. Rodriguez, "Modulated Model Predictive Control for Dynamic Stabilization of DC Microgrid," in *IEEE 11th International Symposium on Power Electronics for Distributed Generation Systems (PEDG)*, 2020, pp. 527–530, doi: 10.1109/PEDG48541.2020.9244405.

[19]   H. Yang, T. Li, Y. Long, C. L. P. Chen, and Y. Xiao, "Distributed virtual inertia implementation of multiple electric springs based on model predictive control in DC microgrids," *IEEE Transactions on Industrial Electronics*, vol. 69, no. 12, pp. 13439–13450, 2022, doi: 10.1109/TIE.2021.3130332.

[20]   J. Zhang, X. Shao, Y. Li, J. Lin, F. Li, and Z. Zhang, "Research on frequency regulation strategy based on model predictive control for wind-hydro-storage complementary microgrid," in *2020 4th International Conference on HVDC (HVDC)*, 2020, pp. 1031–1036, doi: 10.1109/HVDC50696.2020.9292853.

[21]   M. A. Khodja, M. Tadjine, M. S. Boucherit, and M. Benzaoui, "Experimental dynamics identification and control of a quadcopter," in *2017 6th International Conference on Systems and Control (ICSC)*, 2017, pp. 498–502, doi: 10.1109/ICoSC.2017.7958668.

[22]   Zaheeruddin and K. Singh, "Intelligent fractional-order-based centralized frequency controller for microgrid," *IETE Journal of Research*, vol. 68, no. 4, pp. 2848–2862, 2020, doi: 10.1080/03772063.2020.1730249.

[23]   S. Oshnoei, M. Aghamohammadi, and S. Oshnoei, "A novel fractional order controller based on fuzzy logic for regulating the frequency of an islanded microgrid," in *2019 International Power System Conference (PSC)*, 2020, pp. 320–326, doi: 10.1109/PSC49016.2019.9081567.

[24]   S. Khosravi, M. T. H. Beheshti, and H. Rastegar, "Robust control of islanded microgrid frequency using fractional-order PID," *Iranian Journal of Science and Technology, Transactions of Electrical Engineering*, vol. 44, pp. 1207–1220, 2020, doi: 10.1007/s40998-019-00303-6.

[25] Y. Hirase, K. Abe, K. Sugimoto, K. Sakimoto, H. Bevrani, and T. Isse, "A novel control approach for virtual synchronous generators to suppress frequency and voltage fluctuations in microgrids," *Applied Energy*, vol. 210, pp. 699–710, 2018, doi: 10.1016/j.apenergy.2017.06.058.

[26] R. Shi, X. Zhang, C. Hu, H. Xu, J. Gu, and W. Cao, "Self-tuning virtual synchronous generator control for improving frequency stability in autonomous photovoltaic-diesel microgrids," *Journal of Modern Power Systems and Clean Energy*, vol. 6, no. 3, pp. 482–494, 2018, doi: 10.1007/s40565-017-0347-3.

[27] M. Kumar and Y. V. Hote, "Maximum sensitivity-constrained coefficient diagram method-based PIDA controller design: Application for load frequency control of an isolated microgrid," *Electrical Engineering*, vol. 103, pp. 2415–2429, 2021, doi: 10.1007/s00202-021-01226-4.

[28] M. Gheisarnejad and M. H. Khooban, "Secondary load frequency control for multimicrogrids: HiL real-time simulation," *Soft Computing*, vol. 23, no. 14, pp. 5785–5798, 2019, doi: 10.1007/s00500-018-3243-5.

[29] S. Patel, B. Mohanty, and H. M. Hasanien, "Competition over resources optimized fuzzy TIDF controller for frequency stabilization of hybrid micro-grid system," *International Transactions on Electrical Energy Systems*, vol. 30, no. 9, p. e12513, 2020, doi: 10.1002/2050-7038.12513.

[30] B. Khokhar, S. Dahiya, and K. P. S. Parmar, "A robust cascade controller for load frequency control of a standalone microgrid incorporating electric vehicles," *Electric Power Components and Systems*, vol. 48, no. 6, pp. 711–726, 2020, doi: 10.1080/15325008.2020.1797936.

[31] J. Wu, S. Li, Y. Gui, M. Cvetkovic, J. C. Vasquez, and J. M. Guerrero, "Fuzzy Logic-Based Online Energy Management System for Residential Microgrids," in *IECON 2023- 49th Annual Conference of the IEEE Industrial Electronics Society*, 2023, pp. 1–5, doi: 10.1109/IECON51785.2023.10312171.

[32] Z. Zand, S. Khosravi, and M. Hayati, "Design of GaAs-thin film solar cell using TiO_2 hemispherical nanoparticles array," *Optics & Laser Technology*, vol. 156, p. 108608, 2022, doi: 10.1016/j.optlastec.2022.108608.

[33] A. Baldinelli, L. Barelli, G. Bidini, and G. Discepoli, "Economics of innovative high capacity-to-power energy storage technologies pointing at 100% renewable micro-grids," *Journal of Energy Storage*, vol. 28, p. 101198, 2020, doi: 10.1016/j.est.2020.101198.

BIOGRAPHIES OF AUTHORS

Nirdesh Singh received her B.Tech. degree in electrical engineering from Dehradun Institute of Technology, Dehradun, in 2010, M.Tech. degree from Deenbandhu Chhotu Ram University of Science and Technology (DCRUST), Murthal (Sonepat) in 2018, and she is pursuing her Ph.D. in power systems at Deenbandhu Chhotu Ram University of Science and Technology, Murthal (Sonepat). She is an assistant professor at the Department of Electrical Engineering at Ch. Ranbir Singh State Institute of Engineering and Technology (CRS-SIET Jhajjar), Silani Kesho, Jhajjar. Her area of interest is renewable energy systems and power system protection. She can be contacted at email: singh.niru28@gmail.com.

Dr. Dinesh Kumar Jain received his B.Sc. (Engineering), M.Tech., and Ph.D. in electrical engineering from REC Kurukshetra (Now NIT), Haryana, India, in 1987, 1993, and 2001, respectively. He has a total of 35 years of rich academic experience. His area of interest is electrical power quality, power system protection, electric drive, and renewable energy systems. To his credit, he has more than 80 research papers in the international and national journals. He is a professor in the Electrical Engineering Department at Deenbandhu Chhotu Ram University of Science and Technology, Murthal (Sonipat), India. Dr. Jain is a member of ISTE and IEEE. He was awarded the IEEE PES Chapter Outstanding Engineer Award by the IEEE PES IAS Delhi Chapter in 2015. He can be contacted at email: dkjain.ee@dcrustm.org.